

Original Article

STATISTICAL, DIAGNOSTIC AND RESPONSE SURFACE ANALYSIS OF NEFOPAM HYDROCHLORIDE NANOSPHERES USING 3⁵ BOX-BEHNKEN DESIGN

SUKHBIR SINGH^{1,2*}, YASH PAUL SINGLA³, SANDEEP ARORA¹

¹Department of Research, Innovation and Consultancy, Punjab Technical University, Jalandhar-Kapurthala Highway, Kapurthala 144603, Punjab, India, ²Chitkara College of Pharmacy, Chandigarh-Patiala National Highway, Rajpura, Patiala 140401, Punjab, India, ³Lord Shiva College of Pharmacy, Sirsa 125055, Haryana, India
Email: singh.sukhbir12@gmail.com

Received: 28 Jun 2015 Revised and Accepted: 08 Aug 2015

ABSTRACT

Objective: Objective of the current investigation was to analyze effects of operating conditions on characteristics of nefopam hydrochloride nanospheres (NFH-NS). Statistical assessment and diagnostic analysis examined an adequacy and reliability of models.

Methods: NFH-NS were developed by quasi solvent diffusion technique using poly (meth) acrylates by 3⁵ Box-Behnken design. Drug: polymer ratio (X_1), surfactant concentration (X_2), stirring time (X_3), DP/CP Ratio (X_4) and stirring speed (X_5) were selected as independent variables. Response variables investigated were % entrapment efficiency (% EE), mean particle size, % process yield and % drug loading (% DL).

Results: Standardized Pareto chart illustrated that X_1 and X_5 were important factors ($p < 0.05$) affecting response parameters of nanospheres. Significant model F -value ($p < 0.05$) and non-significant lack of fit F -value ($p > 0.05$) epitomized an accuracy of data. Smaller value of predicted residual error sum of squares (PRESS) for regression models stipulated good fit of models. Diagnostic analysis proved normality of data and signified that actual values of response parameters were in agreement with predicted values. Graphical analysis concluded that X_1 , X_2 , X_4 and X_5 had the significant positive effect on % EE. X_1 and X_5 produced remarkable synergistic and antagonistic effect on mean particle size, respectively. X_1 and X_5 exhibited positive effect on % process yield. X_1 produced significant antagonistic effect on % DL.

Conclusion: Optimization report concluded that formulation prepared with 1:3 drug: polymer ratio (w/w), 2 % (w/v) surfactant, 3.8 h stirring time, 1:12 DP/CP ratio and 2000 rpm stirring speed was having highest desirability function of 0.920. Regression models indicated good fit of model, adequate model discrimination and concluded that models can be used to navigate design space.

Keywords: Nefopam hydrochloride, Polyacrylate, Diagnostic analysis, Standardized Pareto chart, Desirability function.

INTRODUCTION

Drug delivery is an interdisciplinary field of investigation and is acquiring the consideration of pharmaceutical researchers [1]. Utmost drugs are constrained by their poor solubility, aggregation due to poor solubility, non-specific delivery, high toxicity, high dosage, *in-vivo* degradation and short circulating half-lives. Nowadays, the field of drug delivery is evolving promptly as researchers from diverse disciplines have joined into support to overcome the drugs ever expanding problems [2].

Nefopam hydrochloride is a non-opioid, non-steroidal, centrally acting analgesic drug having IUPAC name 5-methyl-1-phenyl-1, 3, 4, 6-tetrahydro-2, 5-benzoxazocine hydrochloride [3, 4]. It is the drug of preference for the relief of chronic pain such as cancer pain, nociceptive pain, postoperative pain and neuropathic pain [5-7]. It goes through substantial hepatic pre-systemic metabolism proximately 83%±7, has oral bioavailability approximately 30-40% and an elimination half life of about 3-5 h. The adverse effects of the drug such as nausea, vomiting, dizziness and patient non-compliance limits its application [5, 7].

Design of experiments (DOE) has evolved as powerful, elegant and cost-effective statistical technique which yields more information from fewest runs. Experimental designs are helpful in finding the relative significance of various factors affecting the characteristics of formulation [8-10]. Prerequisite tools needed for DOE include statistical analysis by ANOVA, diagnostic analysis and response surface analysis [11]. The statistical validation involves assessment of statistical parameters such as model F -value, lack of fit F -value, correlation coefficient (R^2), adjusted R-squared (R^2_{Adj}), predicted R-squared (R^2_{Pred}), predicted residual error sum of squares (PRESS) and adequate precision (AP). Model F -value and lack of fit F -value checks for model significance. Correlation coefficient measures amount of variation about the mean. Adjusted R-squared estimates

amount of variation about the mean adjusted for the number of parameters in model. Predicted R-squared enunciates the predictive capability of model. PRESS is the sum of squared differences between the experimental response and predicted response by regression model. PRESS validates how this particular model fits each point in the design. PRESS statistics can be used in the regression model selection. Adequate precision compares the range of predicted values at design points to the average prediction error and measures signal to noise ratio (S/N ratio) [12, 13].

Diagnostics statistics to ensure adequacy and reliability of models. The normal probability plot graphical technique has been used for assessing whether or not the residuals are approximately normally distributed and it should exhibit a strongly linear pattern [14, 15]. The absence of the points in lower and upper extremes of plot indicates that there are not any significant outliers relative to normal distribution. Residual is the difference between the predicted value and an actual value. Residuals have been vital to regression for checking the goodness of data fit in regression line and establishing the credibility of analysis. Studentized residual is the quotient resulting from division of a residual by an estimate of its standard deviation. The studentized residuals have importance in judging outliers in y-direction. Outlier is an observation with large residual. Externally studentized residual vs. predicted plot tests the assumption of constant variance [16, 17]. Externally studentized residual vs. run plot has been used for checking lurking variable that can influence the response during experiment [18]. Predicted vs. actual plots detects how well the model fits the data. For a perfect fit, all the points would be on diagonal [19, 20]. Response surface analysis graphically depicts mathematical relationship between independent and dependent variable in form of response surface plot or contour plot.

Polyacrylate nanospheres of nefopam hydrochloride were prepared by quasi solvent diffusion technique using ratio of two different

grades of poly (meth) acrylates polymer with the quaternary ammonium group to get sustained release of drug [21]. Box-Behnken design response surface methodology was used for design of experiments. The objective of the current investigation was to study effect of operating conditions on response parameters and statistical assessment of the results of experimental design to analyze significance and fitting of model. Diagnostic analysis was performed to check adequacy and reliability of models. Response surface graphical analysis was conducted to generate mathematical relationship in form of the contour plot (2-D) or response surface plot (3-D) between independent and dependent variable. Optimization report was developed by Design-Expert software for determining optimum formulation having the highest desirability function.

MATERIALS AND METHOD

Materials

Nefopam hydrochloride ($C_{17}H_{20}ClNO$, 5-methyl-1-phenyl-1, 3, 4, 6-tetrahydro-2, 5-benzoxazocine hydrochloride, Mw 289.8 g mol⁻¹, CAS

NO-23327-57-3, 99.57 % purity) was procured from Hangz Hou-Daying-Chem. Company Ltd. China. Eudragit RL 100 and RS 100 were received as a gift sample amiably supplied by Evonik Industries AG, Mumbai, India. Acetone (2-Propanone, C_3H_6O , Mw 58.08 g mol⁻¹), Heavy liquid paraffin, n-hexane (C_6H_{14} , Mw 86.18) and were obtained from Merck Specialties Private Limited, Mumbai. Span 80 (sorbitan monooleate, HLB-4.3), Magnesium Stearate (magnesium octadecanoate, 591.27 g mol⁻¹), Sodium hydroxide, Potassium dihydrogen phosphate and Methanol were obtained from Loba Chemicals Private Limited, Mumbai, India. Petroleum ether was purchased from Thomas Bakers Chemical Private Limited, Mumbai. All other chemicals used were of analytical grade.

Experimental design

A 5-factor 3-level Box-Behnken design was established for design of experimentation [22, 23]. The independent and dependent variables used in design are listed in table 1. This study design of 46 experimental runs was generated and analyzed by Design-Expert software (Trial Version 9.0.3.1, Stat-Ease Inc., MN).

Table 1: Variables used in 5-factor 3-level Box-Behnken design using Design-Expert software trial version 9.0.3.1

	Levels		
	Low	Medium	High
Independent variables			
X_1 = Drug: polymer ratio (w/w)	1:2	1:3	1:4
X_2 = Surfactant concentration (% w/v)	0.5	1	2
X_3 = Stirring time (h)	2	3	4
X_4 = DP/CP Ratio (v/v)	1:5	1:10	1:15
X_5 = Stirring Speed (rpm)	1000	1500	2000
Dependent variables Objective			
Y_1 = Entrapment Efficiency (% EE, w/w)			Maximize
Y_2 = Mean Particle Size (nm)			Minimize
Y_3 = Process yield (% w/w)			Maximize
Y_4 = Drug Loading (% DL, w/w)			Maximize

Fabrication of nefopam hydrochloride loaded nanospheres

Polyacrylate nanospheres of nefopam hydrochloride (F1-F46) were prepared by quasi solvent diffusion technique as previously revealed [24]. Accurate quantity of nefopam hydrochloride, eudragit RL 100 and RS 100 was dissolved in acetone-ethanol mixture (DP). Resultant mixture was extruded through syringe #20 slowly to heavy liquid paraffin (CP). Sorbitan monooleate and n-hexane was utilized as surfactant and hardening agent, respectively.

The mixture was continuously stirred with magnetic stirrer (Remi Instruments Division, India) at $38 \pm 0.5^\circ$, centrifuged and washed with petroleum ether. Nanospheres were accumulated by filtration utilizing 0.22 μ m membrane filters followed by ultracentrifugation at 20,000 rpm for 30 min applying cooling centrifuge (RIS-24 BL, Remi Instruments Division, and India) and freeze drying using lyophilizer (ISIC Make, India). A schematic representation of polyacrylate nanospheres of nefopam hydrochloride preparation has been illustrated in fig 1.

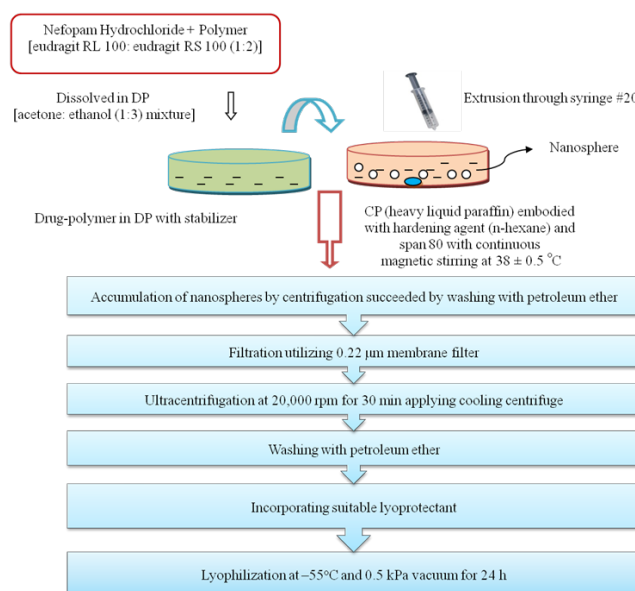


Fig. 1: Schematic representation for fabrication of polyacrylate nanospheres loaded with nefopam hydrochloride

Determination of entrapment efficiency and drug loading

50 mg polyacrylate nanospheres of nefopam hydrochloride (F1-F46) was accurately weighed and extracted with phosphate buffer, pH 7.4 for 24 h followed by centrifugation at 3500 rpm for 10 min. Supernatant was assayed spectrophotometrically at 266 nm using double beam UV spectrophotometer (Systronics AU2701, India). Each measurement was taken in triplicate [25]. NFH concentration was estimated using the calibration curve. The drug entrapment efficiency (% EE, w/w) and drug loading (% DL, w/w) of each formulation of nanosphere was calculated according to Eq. (1) and Eq. (2), respectively.

$$\% EE, w/w = \frac{W_{\text{Entrapped}}}{W_{\text{Drug}}} \times 100 \text{ Eq. (1)}$$

$$\% DL, w/w = \frac{W_{\text{Entrapped}}}{W_{\text{Drug}} + W_{\text{Polymer}}} \times 100 \text{ Eq. (2)}$$

Where, $W_{\text{Entrapped}}$, W_{Drug} and W_{Polymer} were weight of drug entrapped, weight of drug and weight of polymer taken in the system, respectively.

Light microscopy

Mean particle size analysis of polyacrylate nanospheres of nefopam hydrochloride (F1-F46) was conducted under the light microscope with $\times 400$ magnification (Adeltavision Microscopes, India). Images were taken with an APCAM USB2 digital cameras system (APCAM, India) and processed with the Adelta Optec's AP View imaging software. A thin layer of the sample that has been previously diluted with distilled water was spread on microscope slide and viewed under microscope. Samples were measured in triplicate ($n = 3$) and an average value was proclaimed as mean particle size.

Determination of process yield

Weight of dried nanospheres recovered from each run (F1-F46) was weighed accurately. Process yield (% PY, w/w) of nanosphere was calculated using Eq. (3).

$$\% PY, w/w = \frac{W_{\text{Dried nanospheres}}}{W_{\text{Drug}} + W_{\text{Polymer}}} \times 100 \text{ Eq. (3)}$$

Where, $W_{\text{Dried nanospheres}}$, W_{Drug} and W_{Polymer} were weight of dried nanospheres recovered, weight of drug and weight of polymer taken in the system, respectively.

Analysis of experimental data by design-expert software

Standardized pareto chart effect study

The main effect of operating conditions on response parameters was depicted in standardized pareto chart. The length of each bar in chart was proportional to the standardized effect and would be utilized to test the statistical significance of that response parameter. The factors with $p < 0.05$ appeared to be the main factors affecting response parameters.

Statistical analysis

Design-Expert software was used for statistical assessment of the results of experimental design that indulged eminent useful data and asserted the expediency of statistical design for conduct of experiments. The statistical validation was entrenched by assessment of statistical parameters such as model F -value, lack of fit F -value, correlation coefficient (R^2), adjusted R-squared (R^2_{Adj}), predicted R-squared (R^2_{Pred}), predicted residual error sum of squares (PRESS) and adequate precision (AP) generated by ANOVA provision available in the Design-Expert software to check sufficiency and adequacy of models. Model F -value with $p < 0.05$ and lack of fit F -value with $p > 0.05$ for response variables implied that model was significant and the lack of fit was non-significant relative to the pure error, respectively. When the difference between R^2_{Adj} and R^2_{Pred} is less than 0.2, R^2_{Pred} would be in reasonable agreement with R^2_{Adj} . PRESS statistics were used for cross-validation to provide the measure of fit. Regression model with a smaller value of PRESS statistics was preferred. Adequate precision measured signal to noise ratio (S/N ratio). AP value greater than 4 indicated adequate model discrimination. Statistical parameters F -value, R^2 , R^2_{Adj} , R^2_{Pred} , PRESS and AP have been expressed in Eqs. (4)-(11) [26, 27].

$$\text{Mean Square (MS)} = \frac{\text{Sum of Square}}{\text{Degree of freedom}} \text{ Eq. (4)}$$

$$F = \frac{MS_{\text{Regression}}}{MS_{\text{Residual}}} \text{ Eq. (5)}$$

$$R^2 = 1 - \frac{SS_{\text{Residual}}}{SS_{\text{Model}} + SS_{\text{Residual}}} \text{ Eq. (6)}$$

$$R^2_{\text{Adj}} = 1 - \frac{SS_{\text{Residual}}/DF_{\text{Residual}}}{(SS_{\text{Model}} + SS_{\text{Residual}})/(DF_{\text{Model}} + DF_{\text{Residual}})} \text{ Eq. (7)}$$

$$R^2_{\text{Pred}} = 1 - \frac{\text{PRESS}}{SS_{\text{Model}} + SS_{\text{Residual}}} \text{ Eq. (8)}$$

$$\text{Residual} = e_i = [y_i - \hat{y}_i] \text{ Eq. (9)}$$

$$\text{PRESS} = \sum_{i=1}^n [e_i]^2 = \sum_{i=1}^n [y_i - \hat{y}_i]^2 \text{ Eq. (10)}$$

$$\text{AP} = \frac{p\sigma^2}{n} \text{ Eq. (11)}$$

Where, SS is sum of square; DF is degree of freedom; y_i = predicted value; \hat{y}_i = actual value; PRESS is predicted residual error sum of squares; AP is adequate precision; p is the number of model parameters, σ^2 residual mean square, and n is number of experiments.

Diagnostic analysis

Diagnostic plots such as normal probability plot, externally studentized residuals vs. predicted plot, externally studentized residuals vs. run plot and predicted vs. actual plot was developed by Design-Expert software. The normal probability plot was represented between normal % probability and externally studentized residual. Externally studentized residual vs. predicted plot was plotted between externally studentized residual and predicted values of the response parameters [18]. Externally studentized residual vs. run plot was graphically represented between externally studentized residual and order of the experimental run. Predicted vs. actual plots were delineated between predicted and actual response parameter values.

Response surface analysis

The response variables obtained by DoE trials as per study design were suitably modeled to generate graphical depiction of mathematical relationship between independent variables and dependent variable in the form of contour plot (2-D) and response surface graph (3-D) using Design-Expert software [28, 29].

Optimization

Optimization report was developed by Design-Expert software for determining optimum formulation having highest desirability function (Myers et al., 2009).

RESULTS AND DISCUSSION

Standardized pareto chart effect study

Standardized pareto chart effect study was conducted to discover the important factors affecting response parameters of nanospheres. The drug: polymer ratio (X_1), surfactant concentration (X_2) and DP/CP ratio (X_4) had significant positive effect on % EE as revealed by statistical significant p -value ($p < 0.05$) of regression coefficient as shown in standardized pareto chart in fig. 2a. Drug: polymer ratio (X_1) and stirring speed (X_5) exhibited significant synergistic and antagonistic effect on mean particle size, respectively (fig. 2b). Drug: polymer ratio (X_1) and stirring speed (X_5) had the significant synergistic effect on % PY (fig. 2c). Drug: polymer ratio (X_1) manifested significant antagonistic effect on % DL. DP/CP ratio (X_4) and stirring speed (X_5) produced significant synergistic effect on % DL (fig. 2d). From the analysis, it was concluded that drug: polymer ratio (X_1) and stirring speed (X_5) was the important factors affecting response parameters of nanospheres.

Statistical analysis

Analysis of variance (ANOVA) was applied to % EE to study fitting and significance of the model. F -test was carried out to compare regression mean square with residual mean square. Model F -value and lack of fit F -value were found 12.44 ($p < 0.05$) and 1.94 ($p > 0.05$),

respectively which implied that model was significant and lack of fit was non-significant relative to pure error, epitomizing accuracy of data. Non-significant lack of fit indicated good fit of model. Therefore, estimated model may be used for % EE (table 2). Correlation coefficient was 0.9120 which indicated absence of variation about the mean.

Difference between predicted R^2 and adjusted R^2 was found less than 0.2 which indicated rational agreement between regression coefficients. PRESS value was found 642.42 which revealed substantial fit of model. Adequate precision value was found 15.631 which indicated an adequate signal and concluded that model can be used to navigate design space (table 3).

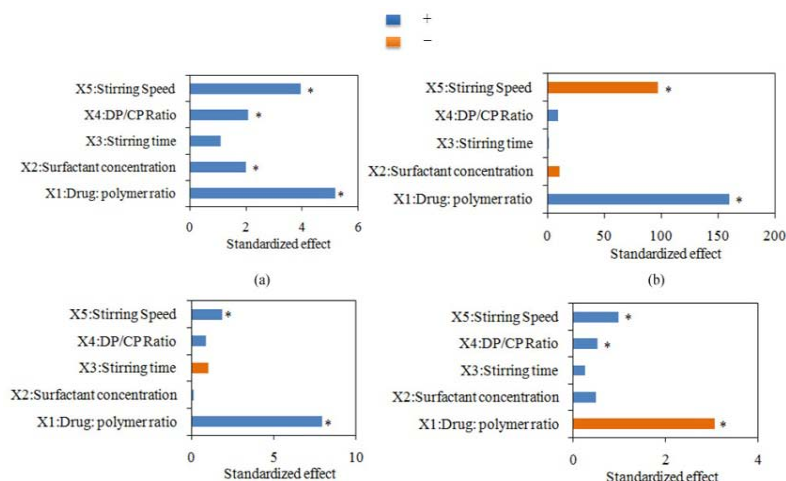


Fig. 2: Standardized Pareto chart for (a) % entrapment efficiency (b) mean particle size (c) % process yield and (d) % drug loading (* significant value $p < 0.05$)

Model generated for mean particle size was found significant as indicated by model F -value 13.71 ($p < 0.05$). Data obtained for mean particle size was acceptable as revealed by non-significant lack of fit F -value 3.82 ($p > 0.05$) (table 2). Predicted R^2 value was found 0.6848 which was in fair agreement with an adjusted R^2 value of 0.8525. PRESS value for mean particle size was perceived $2.583E+005$ which indicated considerable fit of model. An adequate precision value of 16.739 for mean particle size specified fair the signal to noise ratio (S/N ratio > 4) (table 3).

Model generated for % process yield was found significant as indicated by model F -value 13.71 ($p < 0.05$). "Lack of Fit F -value" of 3.00 implied the lack of fit was not significant relative to the pure error (table 2). Predicted R^2 value was found 0.6646 which was in

rational agreement with an adjusted R^2 value of 0.8525. PRESS value for % process yield was found 610.89 which indicated remarkable model fitting. "Adequate Precision" measured signal to noise ratio. S/N ratio was found 14.567 which indicated an adequate signal because ratio greater than 4 was required for adequate model discrimination (table 3).

Model generated for % DL was found significant as indicated by model F -value 25.81 ($p < 0.05$). "Lack of Fit F -value" of 1.84 implies lack of fit was not significant relative to the pure error (table 2). Predicted R^2 value was found 0.8186 which was in fair agreement with an adjusted R^2 value of 0.9186. PRESS value was found 38.42 which indicated significant model fitting. S/N ratio was found 20.384 which revealed an adequate signal (table 3).

Table 2: ANOVA for (a) % entrapment efficiency (b) mean particle size (c) % process yield and (d) % drug loading

Term	Y ₁	Y ₂	Y ₃	Y ₄
	F-Value, p value	F-Value, p-value	F-Value, p-value	F-Value, p-value
Model	12.44, <0.0001*	13.71, <0.0001*	13.71, <0.0001*	25.81, <0.0001*
X ₁	65.46, <0.0001*	148.31, <0.0001*	165.07, <0.0001*	382.43, <0.0001*
X ₂	9.72, 0.0047*	0.68, 0.4184	0.036, 0.8507	10.15, 0.0040*
X ₃	2.89, 0.1022	7.542, 0.9315	2.68, 0.1147	2.81, 0.1065
X ₄	10.60, 0.0034*	0.53, 0.4744	2.02, 0.1678	11.46, 0.0024*
X ₅	38.14, <0.0001*	54.94, <0.0001*	9.24, 0.0056*	40.10, <0.0001*
X ₁ X ₂	7.745, 0.9306	0.48, 0.4935	0.14, 0.7144	4.081, 0.9496
X ₁ X ₃	0.40, 0.5323	1.50, 0.2333	2.10, 0.1603	0.23, 0.6362
X ₁ X ₄	2.586, 0.9599	0.15, 0.6977	0.29, 0.5981	0.25, 0.6195
X ₁ X ₅	0.064, 0.8030	7.91, 0.0096*	1.86, 0.1853	0.054, 0.8188
X ₂ X ₃	1.33, 0.2599	0.31, 0.5835	0.038, 0.8476	1.38, 0.2520
X ₂ X ₄	3.217, 0.9552	2.09, 0.1609	1.71, 0.2035	4.081, 0.9496
X ₂ X ₅	4.957, 0.9445	1.19, 0.2868	0.070, 0.7932	5.165, 0.9433
X ₃ X ₄	0.013, 0.9106	1.42, 0.2443	2.69, 0.1138	0.014, 0.9057
X ₃ X ₅	1.56, 0.2242	0.17, 0.6826	4.15, 0.0528	1.63, 0.2136
X ₄ X ₅	0.96, 0.3370	1.166, 0.9730	0.28, 0.6023	1.01, 0.3244
X ₁ ²	92.74, <0.0001*	18.54, 0.0002*	27.28, <0.0001*	38.72, <0.0001*
X ₂ ²	0.49, 0.4895	0.042, 0.8389	31.69, <0.0001*	0.55, 0.4641
X ₃ ²	2.13, 0.1576	13.13, 0.0014*	0.33, 0.5722	2.48, 0.1282
X ₄ ²	25.02, <0.0001*	8.83, 0.0066*	0.16, 0.6958	27.70, <0.0001*
X ₅ ²	1.98, 0.1723	38.02, <0.0001*	0.25, 0.6189	1.47, 0.2366
Lack of Fit	1.94, 0.2745	3.82, 0.1012	3.00, 0.1479	1.84, 0.2940

*Significant value $p < 0.05$

Table 3: Model statistics of % EE (Y_1), mean particle size (Y_2), % PY (Y_3) and % DL (Y_4)

Parameters	Y_1	Y_2	Y_3	Y_4
R ²	0.9120	0.9195	0.9195	0.9556
Adjusted R ²	0.8387	0.8525	0.8525	0.9186
Predicted R ²	0.6397	0.6848	0.6646	0.8186
PRESS	642.42	2.583E+005	610.89	38.42
Adequate Precision	15.631	16.739	14.567	20.384

Diagnostic analysis

Diagnostic plots were plotted to investigate the goodness of fit of proposed model. Fig. 3a represented the normal probability plot of externally studentized residuals on probit scale which indicated that maximum number of color points depicting value of % EE was located on normal probability line which proved normality of residuals and suggested that response data provided relevant analysis. Normal probability plot indicated whether the residuals

followed normal probability distribution [14]. Fig. 3b illustrated externally studentized residuals vs. predicted values revealed that color points delineating value of % EE were sited within the limits close to zero-axis which sighted the absence of constant error. Fig. 3c explored residual vs. run plot to look for influential variable that may have influenced % EE during the experiment [18]. Predicted vs. actual values plot depicted in fig. 3d revealed that graph was highly linear passing through origin which signified that experimentally observed values of % EE were in close agreement with predicted values [18, 20].

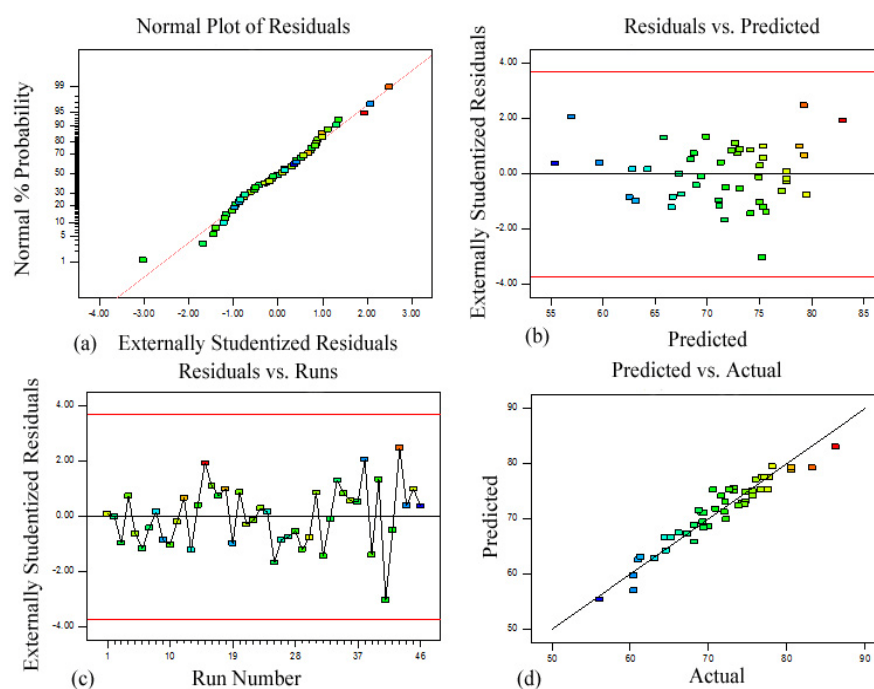


Fig. 3: Diagnostic plot for % entrapment efficiency (a) normal probability plot (b) studentized residuals vs. predicted values plot (c) externally studentized residuals vs. run number plot and (d) predicted vs. actual values plot

Normal plot of studentized residuals represented in fig. 4a indicated that the maximum number of color points depicting mean particle size followed straight line when plotted on probit scale which indicated that response data need not any transformation [14]. Fig. 4b illustrated studentized residuals vs. predicted values which revealed that all color points representing mean particle size had been scattered randomly and uniformly close to zero-axis and had constant range of residual across the graph which illustrated absence of constant variance. Residual versus order of the experimental run for mean particle size were graphically represented in fig. 4c. Random and uniform scatter of points explored absence of lurking variables for mean particle size. Actual vs. predicted plots were plotted between the actual and predicted values of mean particle size for detecting values that cannot be easily predicted by model. Straight line passing from origin revealed that experimentally observed values of mean particle size were analogous with predicted values (fig. 4d).

Normal probability plot of the studentized residuals indicated that maximum number of color points corresponding to % process yield was detected on straight line which proved normality of response

data (fig. 5a). Studentized residuals vs. predicted values plot revealed the absence of megaphone pattern which indicated suitability of % process yield data and absence of constant error (fig. 5b). Fig. 5c explored residual vs. run plot showed random and uniform scatter of color points corresponding to % process yield [18]. Predicted vs. actual values plot revealed most pragmatic information of prognosis that the experimentally observed values of % process yield were analogous with those predicted using optimization methodology (fig. 5d).

Normal probability plot indicated whether the residuals followed normal probability distribution. The maximum number of color points corresponding to % DL plotted on probit scale was sited on straight line as represented in fig. 6a.

Normal plot of residuals deviated from 'S-shaped' curve pattern which suggested that % DL data need not any transformation [14]. fig. 6b illustrated the absence of constant error for % DL. Fig. 6c explored random and uniform scatter of externally studentized residuals for % DL. Fig. 6d manifested that actual values of % DL were in close agreement with predicted values.

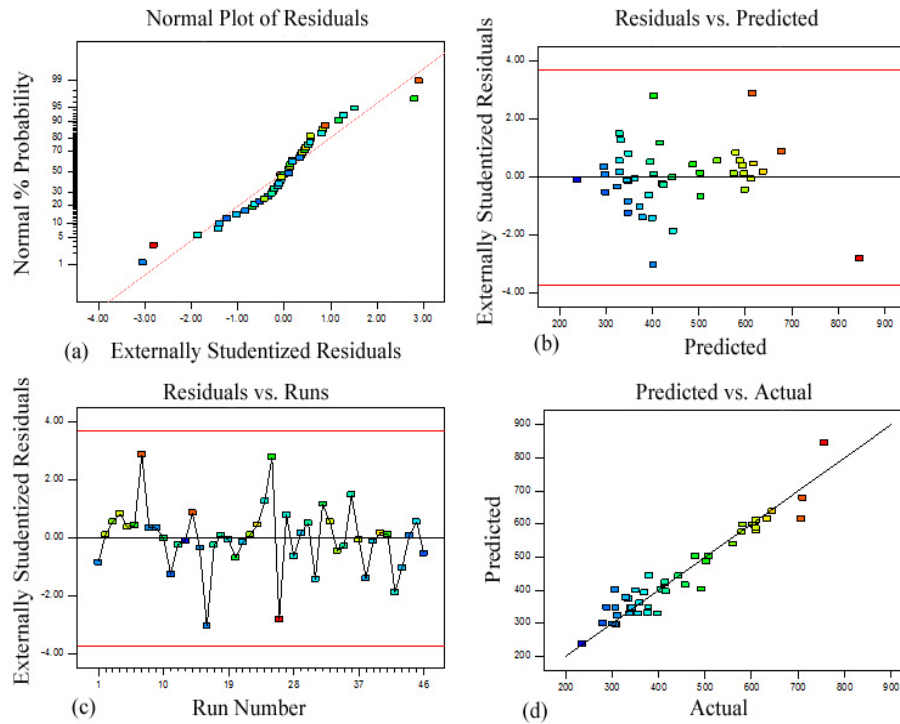


Fig. 4: Diagnostic plot for mean particle size (a) normal probability plot (b) studentized residuals vs. predicted values plot (c) externally studentized residuals vs. run number plot and (d) predicted vs. actual values plot

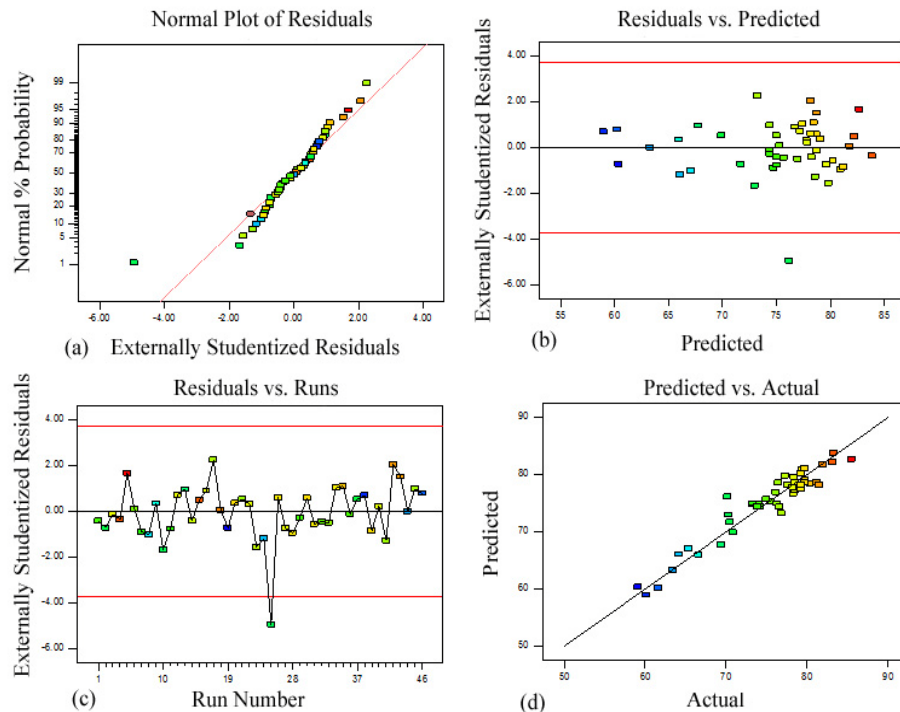


Fig. 5: Diagnostic plot for % process yield (a) normal probability plot (b) studentized residuals vs. predicted values plot (c) externally studentized residuals vs. run number plot and (d) predicted vs. actual values plot

Response surface analysis

Fig. 7a and 8a depicted effect of varying drug: polymer ratio and surfactant concentration on % EE (Y_1) when stirring time, DP/CP ratio and stirring speed was kept steady. Fig. 7b and 8b illustrated influence of varying drug: polymer ratio and stirring time on % EE when surfactant concentration, DP/CP ratio and stirring speed were kept constant. Drug: polymer ratio (X_1) and surfactant concentration

(X_2) indicated significant positive outcome on % EE. This can be due to tremendous amount of polymer available to drug and the increased viscosity of droplets [11, 30, 31]. Entrapment efficiency was significantly increased with an increase in surfactant concentration which can be due to stabilization of emulsion droplets by surfactant [32, 33]. Consequence of varying DP/CP ratio and drug: polymer ratio on % EE was analyzed when other factors were retained fixed as depicted in fig. 7c and 8c.

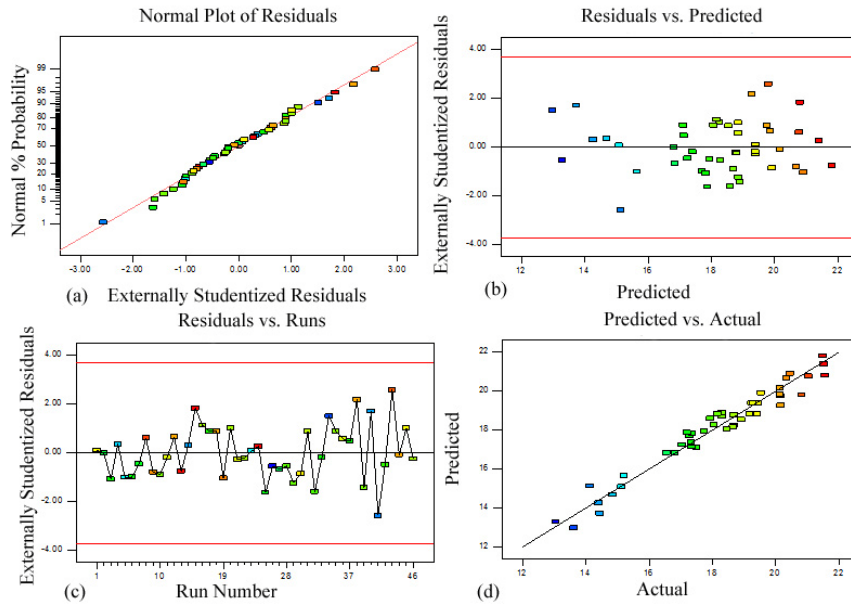


Fig. 6: Diagnostic plot for % drug loading (a) normal probability plot (b) studentized residuals vs. predicted values plot (c) externally studentized residuals vs. run number plot and (d) predicted vs. actual values plot

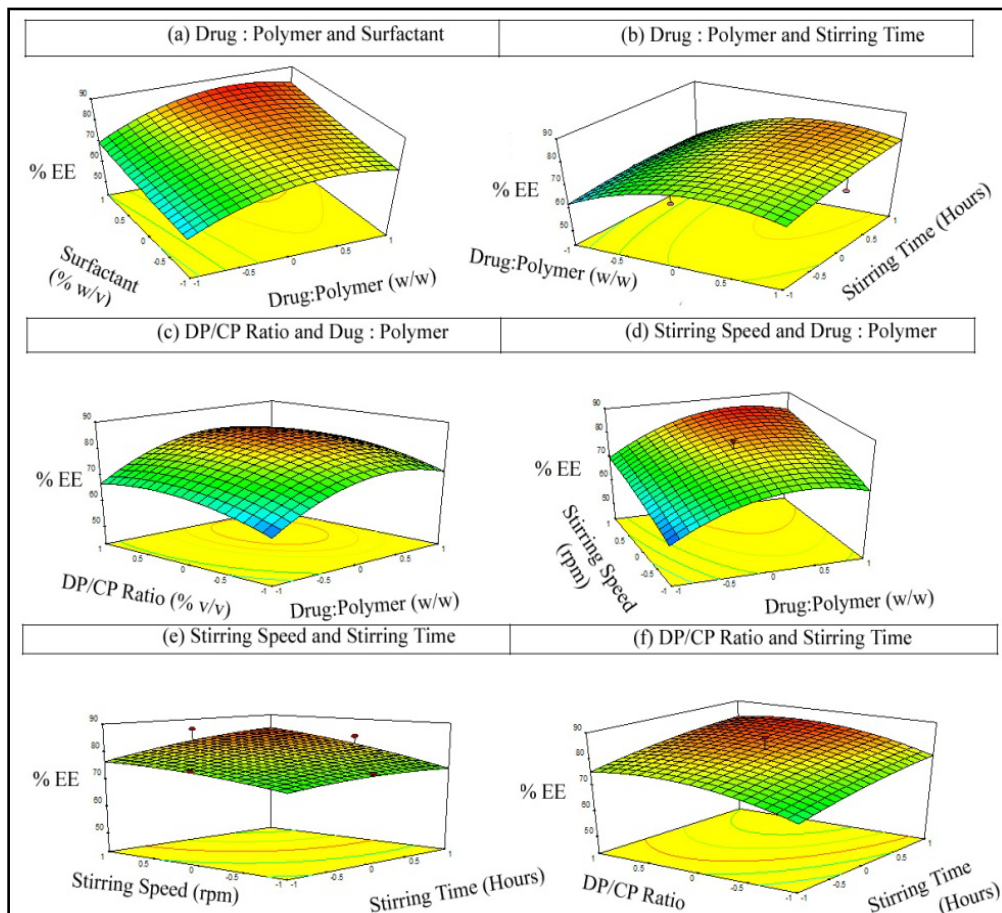


Fig. 7: Response surface plot (3D) showing effect of operating conditions on % EE (Y₁)

DP/CP ratio (X_4) had considerable positive effect on % EE. It had been demonstrated that % EE was remarkably high at medium level of DP/CP ratio due to availability of sufficient amount of CP with adequate viscosity. Effect of changing stirring speed and drug: polymer ratio on % EE (Y_1) was explored as depicted in fig. 7d and 8d. Stirring speed (X_5) had considerable positive impact on % EE. fig. 7e and 8e depicted effect of varying stirring speed and stirring time on % EE. fig. 7f and 8f demonstrated effect of varying DP/CP ratio and stirring time on % EE.

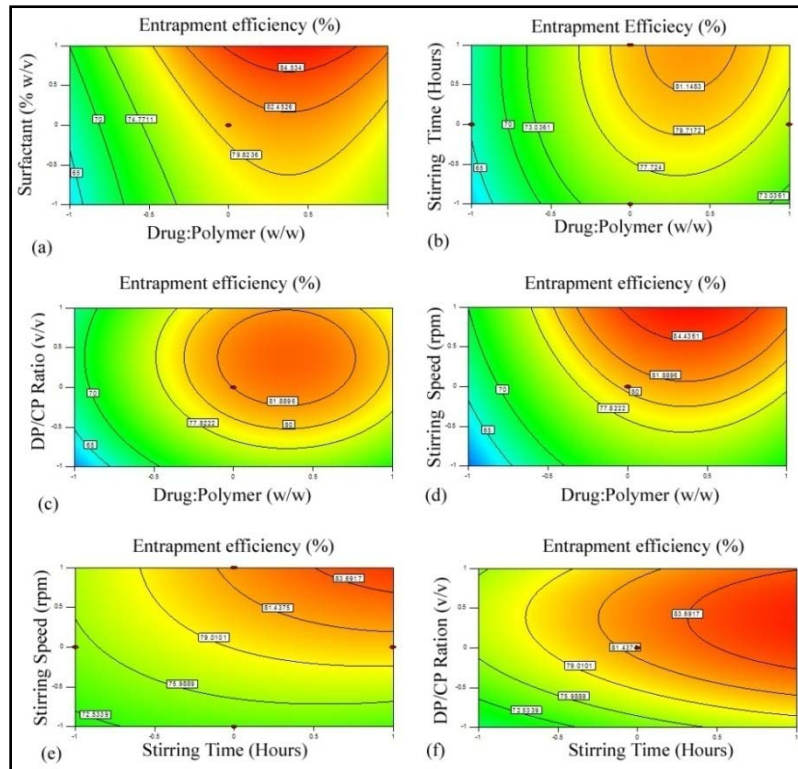


Fig. 8: Counter plot (2D) showing effect of operating conditions on % EE (Y_1)

Effect of transforming drug: polymer ratio (X_1) and stirring time (X_3) on mean particle size (Y_2) was investigated (fig. 9a and 10a). Influence of modifying drug: polymer ratio (X_1) and DP/CP ratio (X_4) on mean particle size (Y_2) was examined (fig. 9b and 10b). It was perceived that mean particle size increased rapidly with increasing drug: polymer ratio which can be illustrated by an increase in density of dispersed phase and size of droplets [11, 30, 31]. Effect of varying drug: polymer ratio (X_1) and stirring speed (X_5) on mean particle size was analyzed (fig. 9c and 10c). Effect of varying stirring time (X_3) and stirring speed (X_5) on mean particle size was studied when other independent variables were retained constant (fig. 9e and 10e).

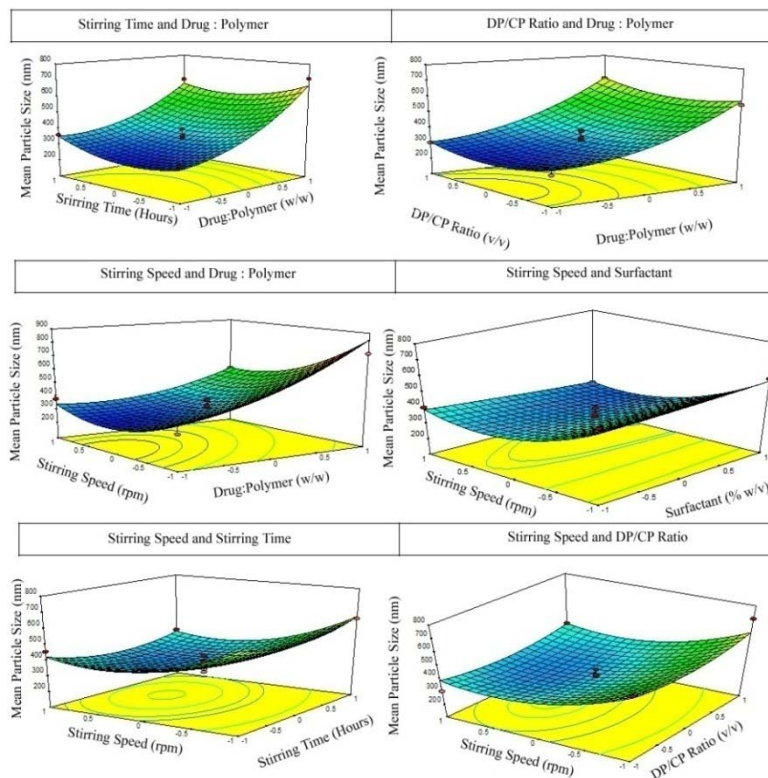


Fig. 9: Response surface plot (3D) showing effect of operating conditions on mean particle size (Y_2)

It was noted that increase in stirring speed resulted in remarkable decrease in mean particle size which can be due to force exerted by high rpm that leads to reduction in particle size [11, 30, 31]. Effect of varying surfactant concentration (X_2) and stirring speed (X_5) on mean particle size was evaluated when drug: polymer ratio, stirring time and DP/CP ratio were kept constant (fig. 9d and 10d). It was observed that increase in surfactant concentration could efficiently reduce the particle size of nanospheres due to surfactant-induced

reduction in surface tension between DP and CP which might stabilize newly generated surfaces and prevents particle aggregation [11, 32-34]. Fig. 9f and 10f demonstrated effect of varying DP/CP ratio (X_4) and stirring speed (X_5) on mean particle size when drug: polymer ratio, surfactant concentration and stirring time were kept constant. Results demonstrated that mean particle size decreased rapidly with increasing stirring speed because high rpm resulted in reduction of particle size [32, 33].

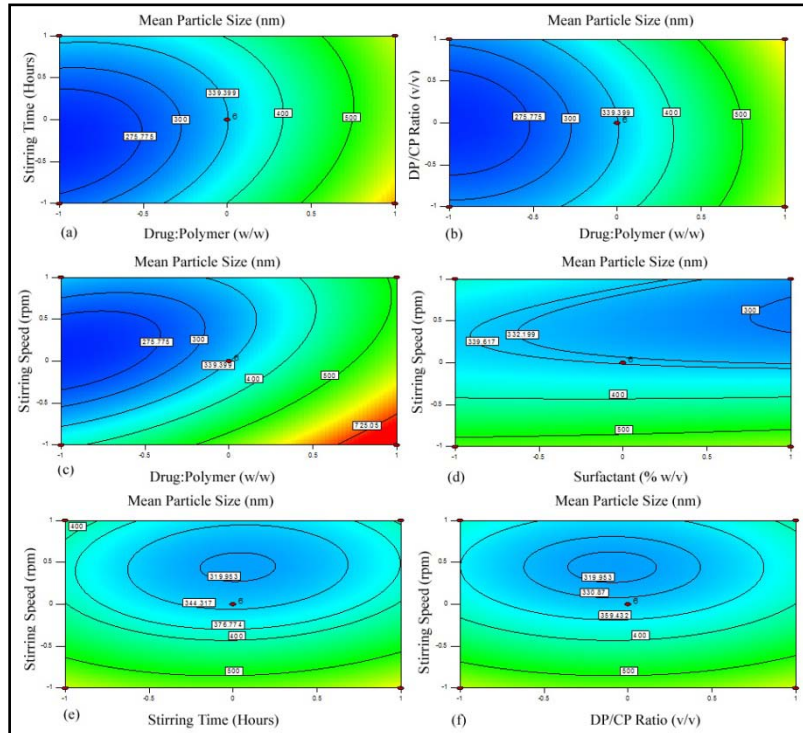


Fig. 10: Counter plot (2D) showing effect of operating conditions on mean particle size (Y_2)

Effect of altering drug: polymer ratio (X_1) on % process yield (Y_3) was reviewed. % process yield increased rapidly with increasing drug: polymer ratio (fig. 11a, 11b, 11c, 12a, 12b and 12c). Influence of modifying stirring time (X_3), DP/CP ratio (X_4) and surfactant concentration (X_2) had no significant effect on % process yield as revealed in response surface graphs and counter plots (fig. 11 and 12).

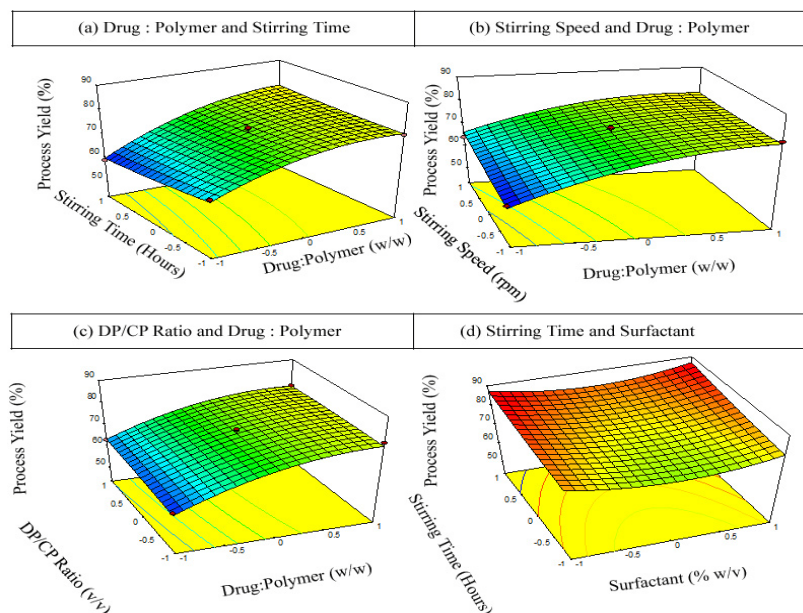


Fig. 11: Response surface plot (3D) showing effect of operating conditions on % process yield (Y_3)

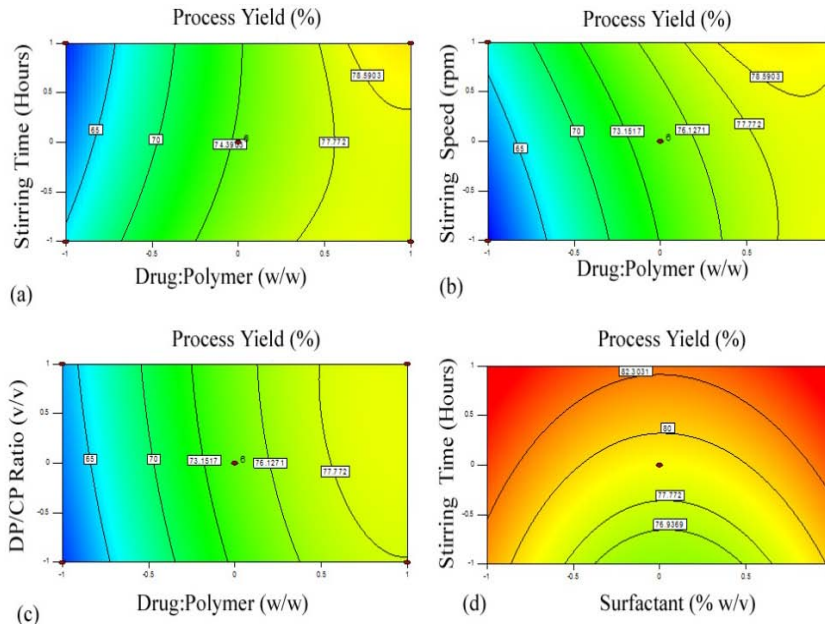


Fig. 12: Counter plot (2D) showing effect of operating conditions on % process yield (Y_3)

Effect of varying drug: polymer ratio (X_1) on % DL (Y_4) was explored and it was observed that % DL decreased rapidly with increasing drug: polymer ratio (fig. 13a, 13b, 13c, 14a, 14b and 14c). Influence of transforming drug: polymer ratio (X_1) and stirring speed (X_5) on % DL was investigated as depicted in fig. 13c and 14c. It was observed that % DL increased with increase in stirring speed.

Effect of changing surfactant concentration (X_2) and DP/CP ratio (X_4) on % DL was examined (fig. 13d and 14d). It was noticed that % DL increased with increase in DP/CP ratio. Stirring time and surfactant concentration had non-significant effect on % DL as revealed in response surface graphs and counter plots (fig. 13 and 14).

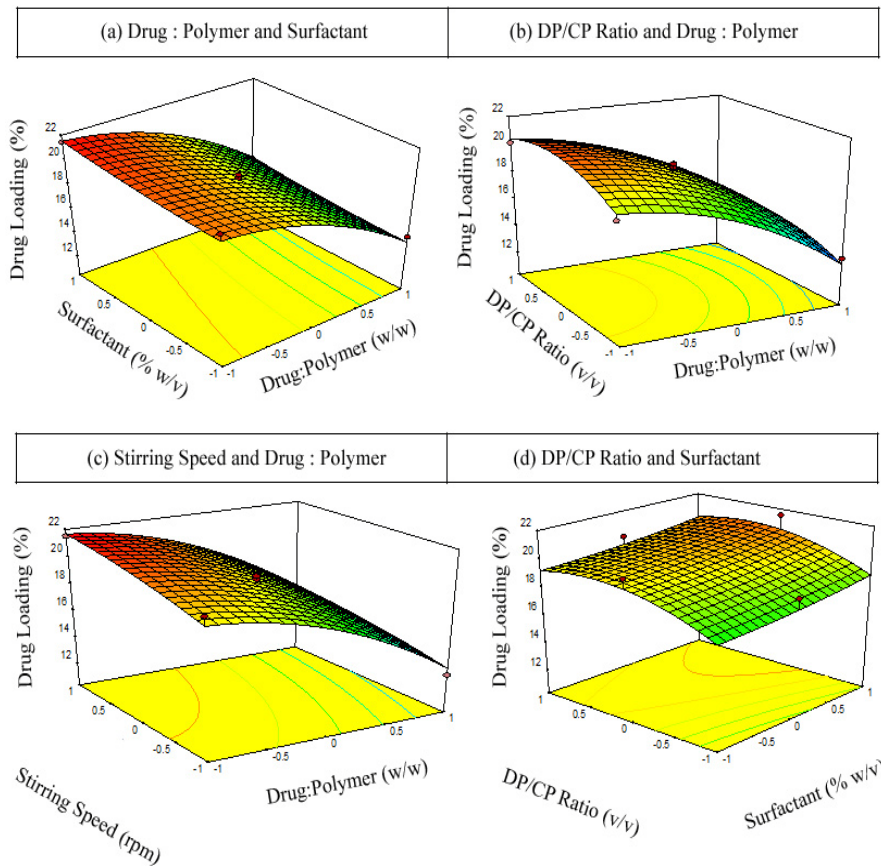


Fig. 13: Response surface plot (3D) showing effect of operating conditions on % DL (Y_4)

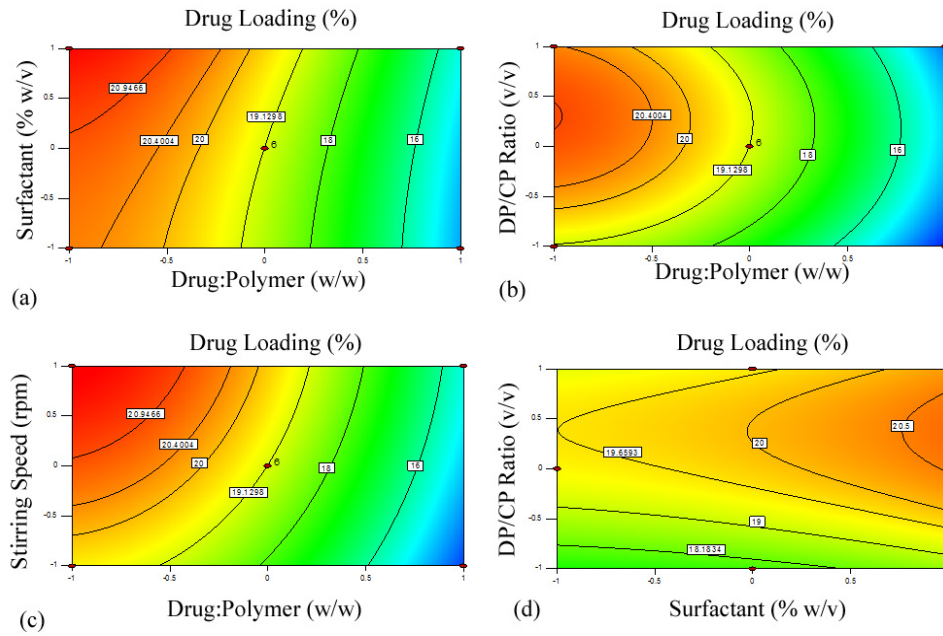


Fig. 14: Counter plot (2D) showing effect of operating conditions on % DL (Y_4)

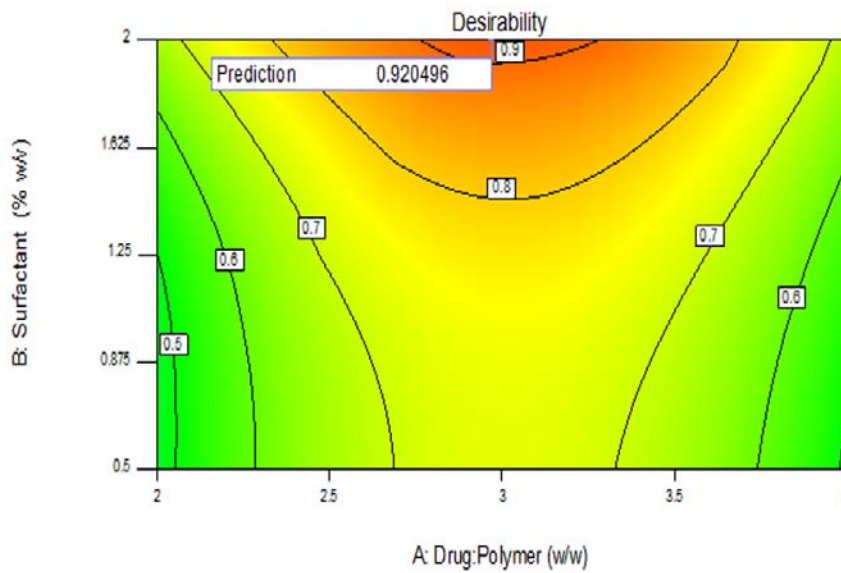


Fig. 15: Counter plot (2D) showing desirability function for optimum formulation predicted by Design-Expert software

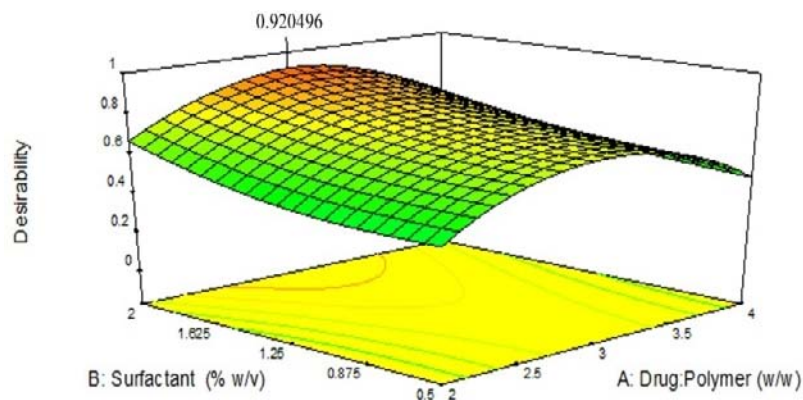


Fig. 16: Response surface plot (3D) showing desirability function for optimum formulation predicted by Design-Expert software

Optimization

Design-expert software developed optimization report which conclude that formulation prepared with 1:3 drug: polymer ratio (w/w), 2 % (w/v) surfactant, 3.8 h stirring time, 1:12 DP/CP ratio and 2000 rpm stirring speed was having highest desirability function of 0.920 (fig. 15 and 16).

CONCLUSION

Polyacrylate nanospheres of NFH were auspiciously fabricated by quasi solvent diffusion technique using 3⁵ Box-Behnken design. This research work conclusively manifested that design of experiments (DoE) has been powerful, elegant and cost-effective statistical technique which yields more information from fewest runs. Standardized pareto chart elucidated that drug: polymer ratio (X_1) and stirring speed (X_5) was substantial factors with $p < 0.05$ affecting response characteristics of nanospheres. Significant model F -value ($p < 0.05$) and non-significant lack of fit F -value ($p > 0.05$) for response variables exemplified accuracy of data. Adjusted R-squared and predicted R-squared indicated rational agreement between regression coefficients. Smaller PRESS value for regression models indicated good fit of model. Adequate precision (AP) value indicated adequate model discrimination and concluded that models can be used to navigate design space.

Normal probability plots proved normality of response data. Externally studentized residuals vs. predicted values of response parameters revealed absence of constant error. Residual vs. run number plot explored absence of lurking variables. Predicted vs. actual values plot revealed that actual values of response parameters were in close agreement with predicted values. Contour plot or response surface plot showed effect of various operating conditions on response parameters in 2-D and 3-D, respectively. It was concluded that X_1 , X_2 , X_4 and X_5 had the significant positive effect on % EE. X_1 and X_5 produced significant synergistic and antagonistic effect on mean particle size, respectively. X_1 and X_5 furnished significant positive effect on % process yield. X_1 produced remarkable antagonistic effect on % DL while X_4 and X_5 exhibited synergistic effect on % DL. Optimization report concluded that formulation prepared with 1:3 drug: polymer ratio (w/w), 2% (w/v) surfactant, 3.8 h stirring time, 1:12 DP/CP ratio and 2000 rpm stirring speed was having highest desirability function of 0.920.

ACKNOWLEDGEMENT

The authors wish to thank Chitkara University for infra structural support of this research study. Authors are grateful to Punjab Technical University for providing access to Science Direct and anti-plagiarism software. The authors also wish to thank Evonik Industries AG, Mumbai, India for providing Eudragit RL 100 and RS 100 as gift sample to carry out this work.

CONFLICT OF INTERESTS

The authors report no conflicts of interest in this work

REFERENCES

- Parveen S, Misra R, Sahoo SK. Nanoparticles: a boon to drug delivery, therapeutics, diagnostics and imaging. *Nanomed: Nanotechnol Biol Med* 2012;8:147-66.
- Orive G, Hernandez RM, Rodriguez GA, Dominguez-Gil A, Pedraz JL. Drug delivery in biotechnology: present and future. *Curr Opin Biotechnol* 2003;14:659-64.
- Alfonsi P, Adam F, Passard A, Guignard B, Sessler DI, Chauvin M. Nefopam-a non-sedative benzoxazocine analgesic selectively reduces the shivering threshold in unanesthetized subjects. *Anesthesiology* 2004;100:37-43.
- Podranski T, Bouillon TW, Riva T, Kurz AM, Oehmke MJ. Compartmental pharmacokinetics of nefopam during mild hypothermia. *Br J Anaesth* 2012;108:784-91.
- Girard P, Pansart Y, Coppé MC, Verniers D, Gillardin JM. Role of the histamine system in nefopam-induced antinociception in mice. *Eur J Pharmacol* 2004;503:63-9.
- Kyung HK, Salahadin A. Rediscovery of nefopam for the treatment of neuropathic pain. *Korean J Pain* 2014;27:103-11.
- Verleye M, André N, Heulard I, Gillardin JM. Nefopam blocks voltage-sensitive sodium channels and modulates glutamatergic transmission in rodent. *Brain Res* 2004;1013:249-55.
- Gohel M, Amin A. Formulation optimization of controlled release diclofenac sodium microspheres using factorial design. *J Controlled Release* 1998;51:115-22.
- Liu C, Wu C, Fang J. Characterization and formulation optimization of solid lipid nanoparticles in vitamin K1 delivery. *Drug Dev Ind Pharm* 2010;36:751-61.
- Nazzal S, Khan M. Response surface methodology for the optimization of ubiquinone self-nanoemulsified drug delivery system. *AAPS PharmSciTech* 2002;3:23-31.
- Jifu H, Xinsheng F, Yanfang Z, Jianzhu W, Fengguang G, Fei Li XP. Development and optimization of solid lipid nanoparticle formulation for ophthalmic delivery of chloramphenicol using a box-behnken design. *Int J Nanomed* 2011;6:683-92.
- Allen DM. The relationship between variable selection and data augmentation and a method for prediction. *Technometrics* 1974;16:125-7.
- Tarpey T. A note on the prediction sum of squares statistic for restricted least squares. *Am Stat* 2000;54:116-8.
- Lewis GA. Optimization methods. In: Swarbrick J, Boylan JC. Eds. *Encyclopedia of pharmaceutical technology*. 2nd ed. New York: Marcel Dekker; 2002. p. 1922-37.
- Norman RD, Harry S. *Applied Regression Analysis*. 2nd ed. New York: John Wiley and Sons; 1981.
- Bolton S. *Pharmaceutical statistics: Practical and clinical applications*. 2nd ed. New York: Marcel Dekker; 1990.
- Singh B, Ahuja N. Development of controlled release buccoadhesive hydrophilic matrices of diltiazem hydrochloride: Optimization of Bioadhesion, dissolution and diffusion parameters. *Drug Dev Ind Pharm* 2002;28:433-44.
- Montgomery DC. *Design and analysis of experiments*. 5th ed. New York: John Wiley and Sons; 2001.
- Montgomery DC. *Design and analysis of experiments*. 7th ed. New York: John Wiley and Sons; 2008.
- Singh B, Agarwal R. Design, development and optimization of controlled release microcapsules of diltiazem hydrochloride. *Indian J Pharm Sci* 2002;64:378-85.
- Ana RCD, Christelle R, Arlette VG, Catarina MMD, Pascale SP. Preparation of acetazolamide composite microparticles by supercritical anti-solvent techniques. *Int J Pharm* 2007;332:132-9.
- Box GEP, Behnken DW. Some new 3 level designs for the study of quantitative variables. *Technometrics* 1960;2:455-75.
- Mandip S, Pankaj D, Viness P, Jayachandra BR. Box-Behnken experimental design in the development of a nasal drug delivery system of model drug hydroxyurea: characterization of viscosity, *in vitro* drug release, droplet size, and dynamic surface tension. *AAPS PharmSciTech* 2005;6:573-85.
- Devarajan PV, Sonavane GS. Preparation and *in-vitro/in-vivo* evaluation of gliclazide loaded eudragit nanoparticles as sustained release carriers. *Drug Dev Ind Pharm* 2007;33:101-11.
- Arindam H, Biswanath S. Preparation and *in-vitro* evaluation of polystyrene-coated (PS-coated) microcapsule of drug-resin complex for achieving prolonged release of diltiazem hydrochloride. *AAPS PharmSciTech* 2006;7:34-49.
- Ahmed AA, Ahmed AE, Ibrahim MAS. Once daily, high-dose mesalazine controlled-release tablet for colonic delivery: optimization of formulation variables using Box-Behnken design. *AAPS PharmSciTech* 2011;12:1454-64.
- Punit PS, Rajashree CM, Yogesh MR, Arti T. Design and optimization of mefloquine hydrochloride microparticles for bitter taste masking. *AAPS PharmSciTech* 2008;9:377-89.
- Lewis GA, Mathieu D, Phan-Tan-Luu R. *Pharmaceutical experimental design*. 1st ed. New York: Marcel Dekker; 1999.
- Myers WR. Response surface methodology. In: Chow, S. C. (Eds.), *Encyclopedia of biopharmaceutical statistics*. New York: Marcel Dekker; 2003. p. 858-69.
- Shah M, Pathak K. Development and statistical optimization of solid lipid nanoparticles of simvastatin by using 2³ full-factorial design. *AAPS PharmSciTech* 2010;11:489-96.

31. Mao S, Shi Y, Li L, Xu J, Schaper A, Kissel T. Effects of process and formulation parameters on characteristics and internal morphology of poly (D, L-lactide-co-glycolide) microspheres formed by the solvent evaporation method. *Eur J Pharm Biopharm* 2008;68:214-23.
32. Gullapalli R, Sheth B. Influence of an optimized non-ionic emulsifier blend on properties of oil-in-water emulsions. *Eur J Pharm Biopharm* 1999;48:233-8.
33. Ko JA, Park HJ, Park YS, Hwang SJ, Park JB. Chitosan microparticle preparation for controlled drug release by response surface methodology. *J Microencapsul* 2004;20:791-7.
34. Yang Y, Chung T, Bai X, Chan W. Effect of preparation conditions on morphology and release profiles of biodegradable polymeric microspheres containing protein fabricated by double-emulsion method. *Chem Eng Sci* 2000;55:2223-36.